AGU PUBLICATIONS

Geophysical Research Letters

RESEARCH LETTER
10.1002/2014GL062279

Key Points:
- Vertical velocities in midlatitude anvil cirrus are ±1 m/s
- Retrieved vertical velocities are low biased
- TKE dissipation rates agree to within 1 order of magnitude

Correspondence to:
A. Muhlbauer,
andreasm@atmos.washington.edu

Citation:
Muhlbauer, A., H. Kalesse, and P. Kollias (2014), Vertical velocities and turbulence in midlatitude anvil cirrus: A comparison between in situ aircraft measurements and ground-based Doppler cloud radar retrievals, *Geophys. Res. Lett.*, *41*, 7814–7821, doi:10.1002/2014GL062279.

Received 20 OCT 2014
Accepted 3 NOV 2014
Accepted article online 7 NOV 2014
Published online 25 NOV 2014

Vertical velocities and turbulence in midlatitude anvil cirrus: A comparison between in situ aircraft measurements and ground-based Doppler cloud radar retrievals

Andreas Muhlbauer[1], Heike Kalesse[2], and Pavlos Kollias[2]

[1] Joint Institute for the Study of the Atmosphere and Ocean, University of Washington, Seattle, Washington, USA, [2] Department of Atmospheric and Oceanic Sciences, McGill University, Montreal, Quebec, Canada

Abstract This study introduces a statistical comparison of vertical velocity observations within cirrus from aircraft and ground-based Doppler cloud radar. Two cases of midlatitude anvil cirrus forming under very similar environmental conditions are examined. The case studies benefit from simultaneous observations of vertical velocities in cirrus collected at and around the Atmospheric Radiation Measurement Southern Great Plains site during the U.S. Department of Energy Small Particles in Cirrus field campaign. Observations from both platforms suggest that the majority of vertical velocities in the examined midlatitude anvil cirrus cases are roughly within ±1 m s^{-1} although higher vertical velocities are occasionally observed. The quality of the vertical velocity comparison between in situ aircraft measurements and ground-based Doppler radar retrievals depends on the case. For the first case on 23 April 2010, the comparison suggests that the radar retrieval may underestimate vertical velocities in the range between roughly 50 cm s^{-1} and 1 m s^{-1}. For the second case on 14 June 2010, the agreement between radar and aircraft is excellent, and the differences are largely within the observed variability of vertical velocities within cirrus. Differences in the spatial scales of vertical velocities and turbulence sampled by the aircraft and Doppler radar, which arise due to differences in the temporal resolution of the observational platforms are not found to explain the observed discrepancies. Estimates for the dissipation rate of turbulent kinetic energy agree to within 1 order of magnitude between the two observational platforms.

1. Introduction

Vertical velocities and turbulence in the upper troposphere are key elements affecting the microphysical properties and dynamical evolution of cirrus clouds. In particular, vertical velocities contribute to the cooling rates in the upper troposphere thereby affecting the values of ice supersaturations, the number concentrations of ice crystals formed by ice nucleation, and the growth rates of ice particles [e.g., *Kärcher and Lohmann*, 2002; *Kärcher and Ström*, 2003]. Adequate parameterizations of the microphysical properties of ice clouds in global climate models (GCMs) require knowledge of the subgrid-scale fluctuations of vertical velocities within a GCM grid box in order to better represent the physical properties and variability of cirrus clouds [e.g., *Kärcher and Lohmann*, 2002]. Thus, a better knowledge of vertical velocities and their mesoscale variability in the upper troposphere is necessary for advancing our understanding of the relationships between large-scale dynamics and the cloud-scale processes that ultimately affect the microphysical and radiative properties of cirrus. However, improving our understanding of the statistical distributions of vertical velocities in the upper troposphere and their relationships to the large-scale environmental conditions requires long-term observations [*Protat and Williams*, 2011].

Until a few years ago, the majority of observations of vertical velocities in cirrus have been collected by aircraft, and this collection of in situ measurements has served as the basis for our present knowledge about the turbulence and wave generating mechanisms controlling the mesoscale variability of vertical velocities in the upper troposphere [e.g., *Scott et al.*, 1990; *Chan et al.*, 1993; *Alexander and Pfister*, 1995; *Gultepe and Starr*, 1995; *Chan et al.*, 1998]. Novel retrieval algorithms are now being used to obtain continuous observations of vertical air motions within cirrus clouds from ground-based profiling Doppler cloud radar [e.g., *Deng and Mace*, 2006; *Kalesse and Kollias*, 2013] although individual efforts to obtain vertical velocities within cirrus from Doppler radar have been made much earlier [e.g., *Heymsfield*, 1975]. Due to their long record and continuous ongoing observations, these radar-based retrievals have the

©2014. American Geophysical Union. All Rights Reserved.

potential to provide an unprecedented amount of data for a wide range of conditions. However, a rigorous comparison of vertical velocities retrievals with in situ aircraft measurements is lacking so far but is necessary for building confidence in the observations and better understanding potential limitations of both observational platforms.

This paper presents a statistical comparison of observed vertical velocities in midlatitude cirrus from aircraft and ground-based Doppler cloud radar. The comparison is conducted for two cases of anvil cirrus observed simultaneously by aircraft and radar at the Southern Great Plains (SGP) site of the U.S. Department of Energy (DOE) Atmospheric Radiation Measurement (ARM) program.

2. Data and Methods

Vertical velocities within cirrus obtained from two different observational platforms are compared in this paper. The aircraft data for this comparison are taken from research flights conducted with the Stratton Park Engineering Company (SPEC Inc.) Learjet 25 aircraft during the U.S. Department of Energy (DOE) Small Particles in Cirrus (SPARTICUS) field campaign. The case studies represent anvil cirrus cloud systems at midlatitudes, which have been sampled by ground-based vertically pointing millimeter wavelength cloud radar (MMCR) [*Kollias et al.*, 2007] at the ARM SGP site and simultaneously by aircraft over or in near proximity to the ARM SGP site in April and June 2010.

2.1. In Situ Aircraft Measurements

In situ measurements of vertical velocities are obtained from the Aircraft-Integrated Meteorological Measurement System (AIMMS-20) instrument fabricated by Aventech Research Inc. and carried aboard the SPEC Inc. Learjet 25 during SPARTICUS. An overview of the basic physical principles and limitations of airborne measurements of air velocities is given in *Lenschow* [1972] and *Scott et al.* [1990]. The AIMMS-20 instrument provides high-resolution measurements of vertical velocities with a sampling rate of 20 Hz. The absolute accuracy of the wind speed measurements is given by the manufacturer as 0.5 m s^{-1} for the horizontal wind components and 0.75 m s^{-1} for the vertical wind component (at 150 knot (approximately 77 m/s) true air speed; http://aventech.com/products/aimms20.html), which is comparable to similar airborne turbulence probes used in other field studies [e.g., *Gultepe et al.*, 1990]. Thus, the absolute accuracy of the vertical velocity measurements is on the same order of magnitude as typically observed vertical velocities in the upper troposphere [*Gultepe et al.*, 1990]. Hence, due to the lack of absolute accuracy, only the perturbation vertical velocity is a reasonably accurate measure and is obtained by removing the bias and linear trend in the aircraft observations similar to previous studies [e.g., *Gultepe and Starr*, 1995; *Muhlbauer et al.*, 2014]. Because sudden aircraft maneuvers can adversely affect the quality of the measurements, all data corrections are performed for flight segments for which the aircraft attitude parameters (i.e., pitch, role, and yaw angles) are approximately constant. Flight segments where changes in the aircraft attitude have a significant effect on the vertical velocity measurements are excluded in this study.

2.2. Doppler Cloud Radar Retrievals

Retrievals of vertical velocities within cirrus are obtained from simultaneous observations of radar reflectivity and Doppler velocity made with the MMCR at the ARM SGP site. The MMCR is a vertically pointing cloud radar operating with a frequency of 35 GHz and capable of measuring radar reflectivities and Doppler velocities with an effective temporal resolution of 10 s and a vertical resolution of 45 m. Deriving vertical air motions from Doppler radar requires decomposition of the vertical velocity profiles obtained from the MMCR Doppler spectrum into reflectivity-weighted fall velocities of hydrometeors (i.e., ice particles) and vertical air motions [*Orr and Kropfli*, 1999; *Mace et al.*, 2002; *Deng and Mace*, 2006; *Protat and Williams*, 2011, and others]. A detailed description of the retrieval technique and processing of the Doppler radar data used in this study is given in *Kalesse and Kollias* [2013]. Here only a brief review of the method is provided below to elucidate the assumptions and limitations of vertical air motion retrievals. The underlying assumptions of the applied methodology is that for sufficiently long averaging times on the order of 5–20 min updrafts and downdrafts within cirrus cancel each other out with averaged vertical air motions close to zero [*Orr and Kropfli*, 1999]. Therefore, for a finite time span, the averaged reflectivity-weighted ice particle fall velocities V_t can be approximated by a power law

$$V_t = aZ^b \tag{1}$$

©2014. American Geophysical Union. All Rights Reserved.

with fit coefficients a and b, and averaged radar reflectivity Z. The power law fit coefficients are then used to determine vertical velocities w (at 10 s temporal resolution) as the difference between the measured Doppler velocities V_d and the reflectivity-weighted fall speeds V_t of ice particles such that:

$$w = V_d - V_t = V_d - aZ^b. \tag{2}$$

The uncertainty of the vertical velocity retrieval is composed of the uncertainty attached to the measurement of Doppler velocities of about 5 cm s^{-1} and the uncertainty arising from the fitted V_t-Z power law relationship, which is on the order of approximately 14 cm s^{-1}. The error in the vertical air motion retrieval is estimated to be on average on the order of 15 cm s^{-1} [*Kalesse and Kollias*, 2013], which is somewhat larger than the uncertainty range of approximately 10 cm s^{-1} given by *Deng and Mace* [2008].

2.3. Turbulent Kinetic Energy Dissipation Rates

Dissipation rates of turbulent kinetic energy (TKE) are computed from the power spectral density of vertical velocity time series. Similar to previous studies [e.g., *Gultepe and Starr*, 1995; *Chan et al.*, 1998; *Kalesse and Kollias*, 2013], we employ Kolmogorov's relationship for isotropic turbulence in the inertial subrange to estimate turbulent dissipation rates from the power spectral density [*Tennekes and Lumley*, 1972]:

$$\Phi(\kappa) = \alpha\epsilon^{2/3}\kappa^{-5/3}. \tag{3}$$

Here $\Phi(\kappa)$ is the one-dimensional power spectral density of vertical velocity as a function of wave number κ and α is the Kolmogorov constant. The wave number κ is related to frequency f such that $\kappa = 2\pi f/U$, where U is the ambient wind speed at cirrus altitude in case of ground-based radar observations or the true air speed in case of the aircraft measurements. For the Kolmogorov constant, we use a value of $\alpha = 0.53$, which is appropriate for atmospheric flows in the upper troposphere or other geophysical flows with sufficiently large Reynolds numbers [*Sreenivasan*, 1995] and for one-dimensional energy spectra derived from a single wind component. The turbulent kinetic energy dissipation rates can be derived by solving equation (3) for ϵ, which yields

$$\epsilon = \left[\frac{2\int_{\kappa_1}^{\kappa_2}\Phi(\kappa)\mathrm{d}\kappa}{3\alpha\left(\kappa_1^{-2/3} - \kappa_2^{-2/3}\right)}\right]^{3/2}. \tag{4}$$

The term $\int_{\kappa_1}^{\kappa_2}\Phi(\kappa)\mathrm{d}\kappa$ can be estimated from the observations by integrating the power spectral density $\Phi(\kappa)$ over a range of wave numbers $[\kappa_1, \kappa_2]$ within the inertial subrange. For the aircraft observations, we loosely follow *Chan et al.* [1998] and use a frequency range of 0.8 Hz to 5 Hz for integrating the power spectral density in the inertial subrange. Assuming a true air speed of about 220 m s^{-1}, the frequency bounds are equivalent to horizontal length scales between 40 m and 275 m. The upper frequency bound is chosen somewhat lower than the Nyquist frequency, which is 10 Hz in the case of the aircraft observations. Since the sampling rate of the radar is much lower than aircraft sampling rate, we extrapolate the power spectral density seen by the radar to higher frequencies by linearly regressing the power spectral densities as a function of the wave number in log-log space. Energy dissipation rates from the Doppler radar observations are then calculated in the same fashion as the aircraft data by integrating over the extrapolated power spectral densities. This procedure is only performed if the theoretically expected −5/3 spectral slope is established in the radar observations and contained within the 95% confidence intervals of the spectral slope estimated by the linear model. The power spectral density is computed from the time series of vertical velocities (from aircraft and radar) by means of discrete Fourier transformation. The Welch's method [*Welch*, 1967] is employed for the estimation of power spectral densities from the vertical velocity time series; that is, the original time series is split up into overlapping segments, and each segment is windowed using a Hamming window function. The power spectral density estimates are then averaged over each segment. Thus, the application of Welch's method reduces the overall variance of the spectrum in exchange for a reduction in the frequency resolution.

3. Case Studies

In the subsequent section we discuss two cases of midlatitude anvil cirrus observed simultaneously by aircraft and ground-based radar at the ARM SGP site in April and June 2010 during the SPARTICUS field campaign.

©2014. American Geophysical Union. All Rights Reserved.

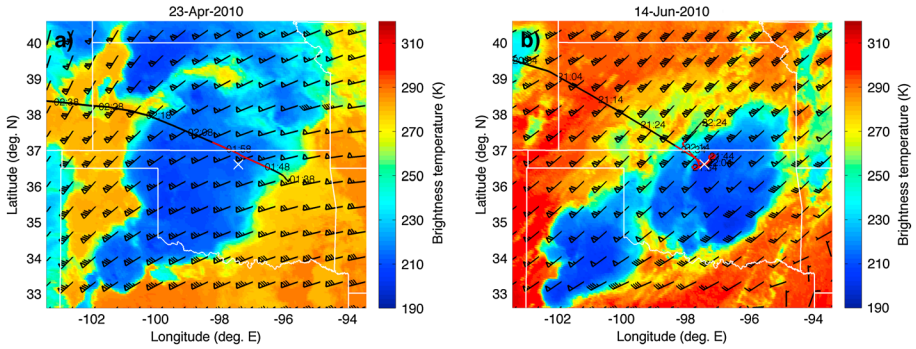

Figure 1. Schematic overview of the anvil cirrus cases sampled by aircraft on (a) 23 April 2010 and (b) 14 June 2010. Shown are the brightness temperature (shaded) in the 10.7 μm channel from GOES satellites at 02:15 UTC and 22:15 UTC, respectively, the aircraft flight track (black) and the portion of the flight track used for the comparison (red). Upper level wind speeds and direction at the 200 hPa pressure level are taken from the European Centre for Medium-Range Weather Forecasts ERA-Interim reanalysis and are shown for 00 UTC. Flags represent 50 knots, full barbs represent 10 knots, and half barbs represent 5 knots. State boundaries and the location of the ARM SGP site are shown as thin white lines and white cross, respectively.

3.1. Meteorological Overview

Both anvil cirrus cases originate from deep convective systems forming close to the boarder region between northern Texas and the southern parts of Oklahoma. In the 23 April 2010 anvil cirrus case, deep convection is triggered along a line of convergence forming as a result of southwesterly flows impinging a southeasterly low-level influx of warm and moisture-laden air from the Gulf of Mexico. The anvil cirrus is then influenced by the southwesterly flows at upper levels and advects over the ARM SGP site. The 14 June 2010 anvil cirrus case forms under very similar synoptic conditions featuring a convergence line in the southwestern parts of Oklahoma resulting from the confluence of southeasterly and northwesterly flows at low levels and a relatively strong southwesterly flow at upper levels (up to 35 m s^{-1} at about 12.5 km height).

Figure 1 gives a schematic overview of the horizontal extent of the anvil cirrus cases relative to the location of the ARM SGP site and the aircraft flight tracks. The research flight conducted on 23 April 2010 started out in Tulsa (OK), where the aircraft was stationed during the day, and continued on an outbound track back to Boulder (CO) where the aircraft was based during the SPARTICUS campaign. The aircraft departed from Tulsa airport at around 01:45 UTC and sampled the anvil cirrus en route from cloud base to top between 01:48 UTC and 02:18 UTC in a series of ascents and ramped level legs on a relatively straight flight track (Figure 1a). On 14 June 14 2014, the Learjet departed in Boulder at 20:37 UTC and sampled anvil cirrus over the ARM SGP site in a series of horizontal flight legs and ramped ascents/descents before heading toward Wichita (KS) where the aircraft landed at approximately 22:30 UTC (Figure 1b).

3.2. Cloud Profiles

Time-height sequences of radar reflectivity profiles from the MMCR at the ARM SGP site are shown in Figures 2a and 2b for both anvil cirrus cases. The cirrus anvils are sampled by the MMCR for a 1 h long period approximately centered around the aircraft sampling time. During 01:30 UTC and 02:30 UTC on 23 April 2010, the radar reflectivity profiles indicate a relatively horizontally homogeneous anvil cirrus cloud with increasing radar reflectivity toward cloud base. The increase in radar reflectivities toward cloud base is indicative of larger ice particles with larger ice fall speeds and likely a result of size sorting effects of the sedimenting ice particles as they grow by vapor deposition and aggregation. The decrease of radar reflectivities toward the radar echo base is indicative of a decrease in ice particle size due to sublimation in the subsaturated air below cloud base. However, the anvil cirrus slowly deepens over time with cloud base height dropping from 8 km down to about 6.5 km and cloud top rising from slightly below 12 km height to almost 12.5 km (Figure 2a). The deepening of the anvil cloud layer and the lowering of the cloud base height may be explained by the sublimation of precipitating ice particles leading to diabatic cooling and potentially to a destabilization of the cloud layers near cloud base and the promotion of buoyancy instabilities [e.g., *Harris*, 1977]. Temperatures range between −60°C at cloud top and −25°C at cloud base.

©2014. American Geophysical Union. All Rights Reserved.

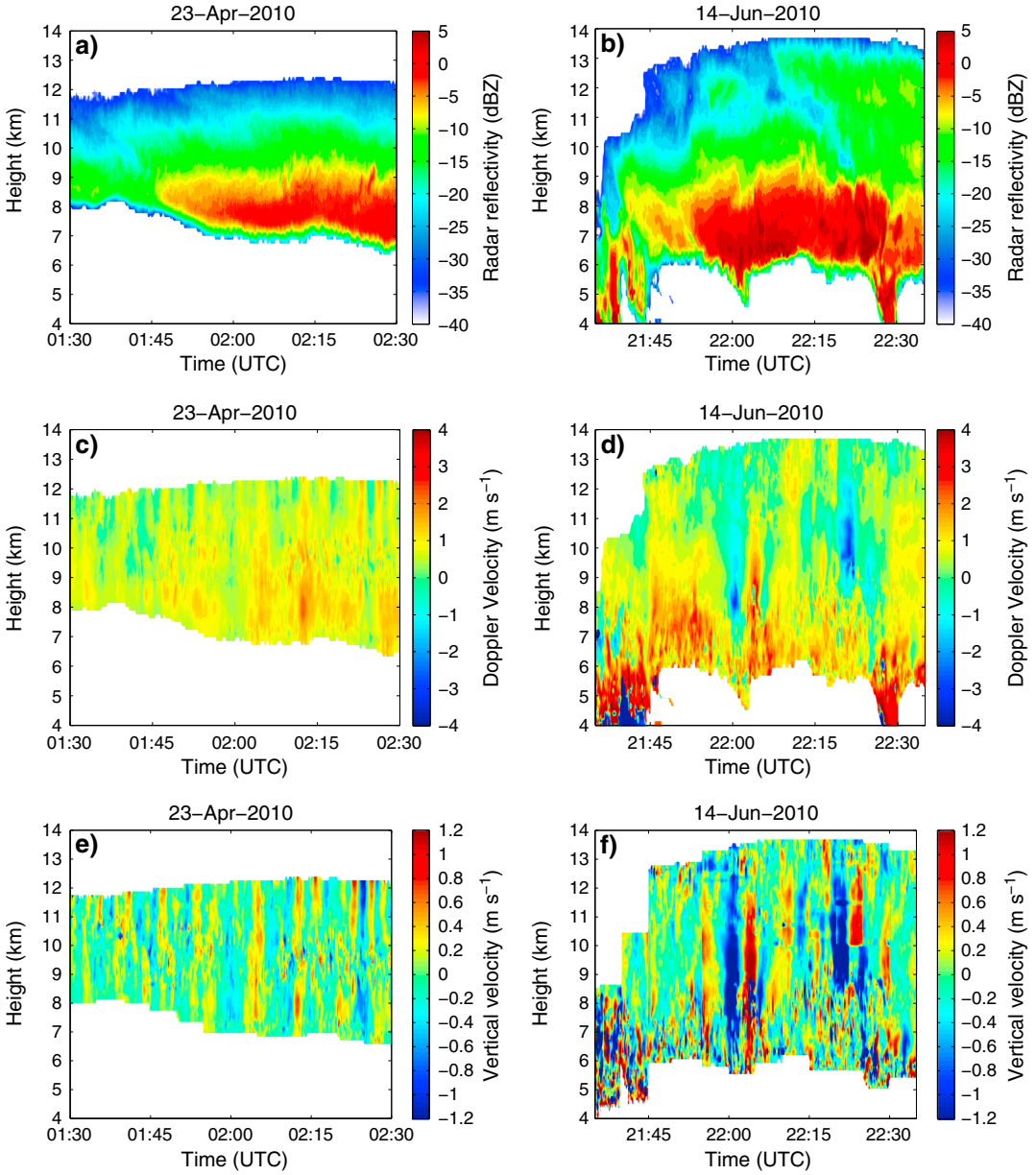

Figure 2. Time-height plot of (a, b) MMCR radar reflectivity, (c, d) Doppler velocities, and (e, f) vertical velocity retrieval for the 23 April (Figures 2a, 2c, and 2e) and 14 June anvil cirrus case (Figures 2b, 2d, and 2f). Note that positive velocities correspond to downward air motion.

The observed Doppler velocities and retrieved vertical velocities within the anvil cirrus cloud are shown in Figures 2c–2f, respectively. During the second half of the observational period, as the anvil cirrus deepens, the intensity of vertical velocities increases near cloud base, which may be caused by the diabatic cooling induced by the sublimating ice particles. Toward the top of the anvil cirrus, the repetitive pattern of columns of updrafts and downdrafts in particular toward the end of the time series may be indicative for propagating internal gravity waves (Figures 2c and 2e). The anvil cirrus sampled between 21:35 UTC and 22:35 UTC on 14 June 2010 is considerably thicker and ranges from roughly 6 km to 13.5 km height. Although the vertical structure of the radar reflectivity profiles is qualitatively similar to the 23 April anvil cirrus case, the radar reflectivities toward cloud base are considerably higher with values up to about 5 dBZ indicating larger ice crystals as in the previous case (Figure 2b). Similar to the previous case, cloud top temperatures are approximately −60°C, but cloud base temperatures are considerably warmer at around −10°C suggesting that ice

©2014. American Geophysical Union. All Rights Reserved.

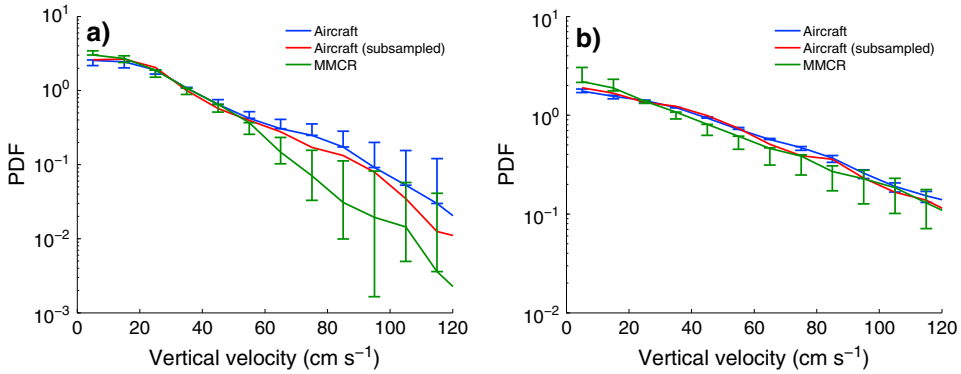

Figure 3. Probability density functions (PDF) of absolute values of vertical velocities within cirrus observed by the aircraft (blue) and retrieved from the MMCR observations (green) for the anvil cirrus cases on (a) 23 April 2010 and (b) 14 June 2010. The PDF of aircraft data subsampled at the same rate as the MMCR is shown as solid red line. The uncertainty range is indicated by the vertical extent of the bars. For the aircraft data, the uncertainty range reflects the variability of the PDF generated by sampling aircraft data within a 50 km, 100 km, and 200 km radius around the ARM SGP site. For the radar data, the uncertainty range reflects the variability generated by sampling from the first and the second half of the 1 h long time interval. Note the change in scale of the *y* axis in Figure 3b.

aggregation may play a more important role in the lower parts of the anvil cirrus by promoting ice particle growth to larger sizes. The profiles of observed Doppler velocities and retrieved vertical velocities in cirrus (Figures 2d and 2f) show broad and deep regions of updrafts and downdrafts (e.g., at around 22:00 UTC and after 22:15 UTC). Some small-scale but highly active turbulent features are also evident at cloud top and base, and the turbulence at cloud base is much stronger than for the 23 April case.

3.3. Vertical Velocities and Energy Dissipation Rates

A comparison of the probability density functions (PDFs) of the absolute values of vertical velocities observed by the two different platforms is shown in Figure 3. For this comparison, we only consider aircraft data collected at heights above the anvil cirrus cloud base, within the same cloud system as determined by visually assessing the aircraft location with respect to the location of the cloud fields seen by GOES satellites (Figure 1) and within a predefined maximum distance of 100 km between the aircraft and the ARM SGP site. Because these constraints are subjective and may introduce appreciable uncertainty for the statistical aircraft-radar comparison and the variability of the vertical velocity PDF, we construct uncertainty bounds of the vertical velocity PDF by varying the maximum allowed horizontal aircraft-radar distance between 50 km and 200 km. This uncertainty range is indicated by the error bars attached to the aircraft-derived vertical velocity PDFs in Figure 3 and gives a first-order estimate of how the sampling uncertainty affects the variability of the PDF. Similarly, an uncertainty range is constructed for the vertical velocity retrievals from the radar by sampling only the first and second half of the data.

For the 23 April case, both the in situ aircraft observations and the vertical velocities retrieved from cloud profiling Doppler radar agree well for the lower range of vertical velocities up to about 50 cm s^{-1}. However, the occurrence frequency for vertical velocities larger than about 50 cm s^{-1} is systematically lower in the Doppler radar retrievals than in the in situ measurements taken by the aircraft, and there is little to no overlap between the uncertainty ranges. For vertical velocities larger than about 50 cm s^{-1}, the discrepancy between the aircraft observations and the retrievals increases with increasing vertical velocity up to 1 order of magnitude for vertical velocities in the range of 1 m s^{-1} and larger. A possible explanation for the discrepancy between the aircraft observations and the radar retrievals may be that vertical velocities larger than about 50 cm s^{-1} may originate from small-scale eddies or high-frequency gravity waves with wavelengths not resolved by the radar sampling volume. We tested this hypothesis by subsampling the aircraft data with the same horizontal resolution as the radar but find that differences in the sampling length scale between the aircraft and radar platform contribute relatively little to the overall discrepancies but become more important toward the high vertical velocity tail of the PDF (Figure 3a). The underestimation of the occurrence frequencies of low ($\leq$ 10 cm s^{-1}) vertical velocities may be due to the well-known sampling limitation of aircraft data particularly for low-frequency gravity waves with wavelengths exceeding the typical length of flight legs.

©2014. American Geophysical Union. All Rights Reserved.

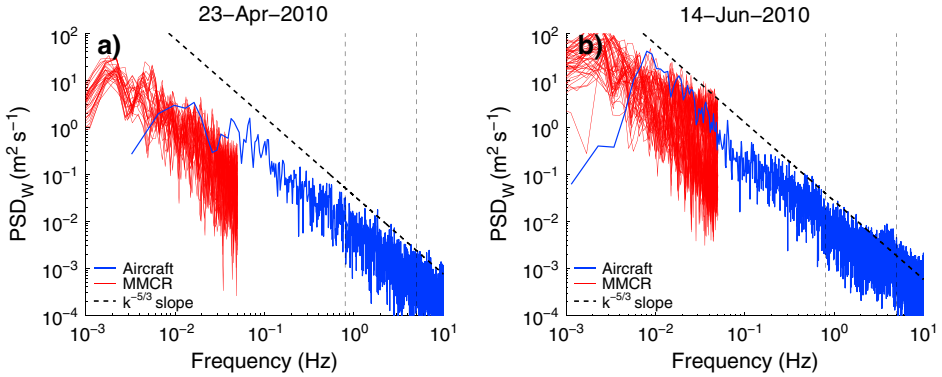

Figure 4. Power spectral density (PSD) of vertical velocities from aircraft (blue) and MMCR (red) for the anvil cirrus case on (a) 23 April 2010 and (b) 14 June 2010. The theoretically expected $k^{-5/3}$ spectral slope is shown for reference (thick dashed). The frequency range 0.8 Hz to 5 Hz used in the calculation of the turbulent dissipation rates is indicated by the vertical lines (thin dashed).

For the 14 June anvil cirrus case, the overall agreement between the aircraft and radar vertical velocity data is very good. Again, there is indication for the aircraft measurements to underestimate at the small vertical velocities range of the PDF and for the radar-based vertical velocity retrievals to slightly underestimate vertical velocities in the range between roughly 50 cm s^{-1} and 80 cm s^{-1}. However, throughout most of the range of the PDF, vertical velocities agree to within the sampling variability and uncertainty induced by the spatial separation between the aircraft and the radar (Figure 3b). Figure 4 shows a comparison of the power spectral densities derived from the aircraft and radar data. At low frequencies of about 0.01 Hz, the power spectral densities observed by radar and aircraft are overlapping, which suggests that both the radar and the aircraft observe similar contributions of vertical velocities from the gravity wave spectrum. However, at higher frequencies, the power spectral densities estimated from the aircraft data are considerably higher than the ones extrapolated from the radar observations (not shown). Also, at the very low frequency end of the spectrum, the energy contributions seen by the radar are larger than for the aircraft data which taper off at low frequencies. The lack of spectral power at the low-frequency range in the aircraft measurements is consistent with the underestimation of the occurrence frequency of low vertical velocities seen in Figure 3.

The dissipation rates for turbulent kinetic energy obtained from the aircraft data are on the order of 9.7×10^{-5} m^2 s^{-3} for the 23 April anvil cirrus case and 1.5×10^{-4} m^2 s^{-3} for the 14 June anvil cirrus case, which is consistent within the relatively broad range of TKE dissipation rates in cirrus of 0.5×10^{-4} m^2 s^{-3} to 8×10^{-4} m^2 s^{-3} reported from previous aircraft measurements [*Quante and Starr*, 2002]. The averaged TKE dissipation rates obtained from the radar retrievals are 1.2×10^{-5} m^2 s^{-3} (23 April 2010) and 3.8×10^{-4} m^2 s^{-3} (14 June 2010) and, thus, are comparable to the aircraft data to within 1 order of magnitude at least (see Table 1 for details). In particular, the discrepancy between the radar retrievals and the in situ measurements is smaller than the approximately 4 to 5 orders of magnitude observed natural variability of TKE dissipation rates in the upper troposphere [e.g., *Gultepe and Starr*, 1995; *Chan et al.*, 1998; *Quante and Starr*, 2002].

Table 1. Dissipation Rates ϵ of Turbulent Kinetic Energy (TKE) Derived From In Situ Aircraft and Doppler Radar Observations for Two Cases of Anvil Cirrus Observed During SPARTICUS[a]

Case Study	Cirrus Type	ϵ (Aircraft) (m^2 s^{-3})	ϵ (Radar) (m^2 s^{-3})
23 April 2010	Anvil cirrus	9.7×10^{-5}	1.2×10^{-5} (3.0×10^{-6}, 5.2×10^{-5})
14 June 2010	Anvil cirrus	1.5×10^{-4}	3.8×10^{-4} (1.1×10^{-5}, 1.5×10^{-3})

[a]The 95% confidence intervals for the TKE dissipation rates obtained from Doppler radar are given in parentheses.

©2014. American Geophysical Union. All Rights Reserved.

4. Summary and Conclusions

This study introduces a statistical comparison of vertical velocity observations within cirrus from aircraft and ground-based cloud profiling Doppler radar. Two cases of midlatitude anvil cirrus forming under very similar environmental conditions are examined. The case studies benefit from simultaneous observations of vertical velocities in cirrus collected at and around the ARM SGP site during the SPARTICUS field campaign. Observations from both platforms suggest that the majority of vertical velocities in the examined case studies of midlatitude anvil cirrus are roughly within ± 1 m s^{-1} although higher vertical velocities are occasionally observed. The quality of the vertical velocity comparison between in situ aircraft measurements and ground-based Doppler radar retrievals depends on the case. For the first case on 23 April 2010, the comparison suggests that the radar retrieval may underestimate vertical velocities in the range between roughly 50 cm s^{-1} and 1 m s^{-1}. For the second case on 14 June 2010, the agreement between radar and aircraft is excellent and the differences are smaller than the observed spatial variability of vertical velocities within cirrus as explained by the spatial distance between the aircraft and the radar. Differences in the spatial scales of vertical velocities and turbulence sampled by the aircraft and Doppler radar, which arise due to differences in the temporal resolution of the observational platforms are not found to explain the observed discrepancies. Estimates for the dissipation rate of turbulent kinetic energy agree to within 1 order of magnitude between the two observational platforms. The comparison suggest that retrievals of vertical velocities have considerable potential for providing high-quality continuous observations of vertical velocities in the upper troposphere, but further comparisons and dedicated campaigns are necessary to further investigate the discrepancies and to better understand the effect of the microphysical assumptions on the vertical velocity retrievals.

Acknowledgments

We gratefully acknowledge R. Paul Lawson and Ted Fisher (SPEC Inc.) for providing the AIMMS-20 data at 20 Hz time resolution, Patrick Minnis (NASA LaRC) for providing the GOES data and the ARM program of the U.S. Department of Energy (DOE) for providing the MMCR data. All data used in this manuscript are available from the first author upon request (Andreas Muhlbauer, andreasm@atmos.washington.edu). We greatly appreciate the effort of the SPARTICUS science team (Jay Mace, Thomas Ackerman, Jennifer Comstock, Tim Garrett, Eric Jensen, Xiaohong Liu, Greg McFarquhar, and David Mitchell) who devoted much of their time to make the SPARTICUS field campaign a success. Andreas Muhlbauer acknowledges funding received from NSF grant 1144017. Heike Kalesse and Pavlos Kollias acknowledge funding from the U.S. DOE Atmospheric System Research (ASR) program. The publication is partially funded by the Joint Institute for the Study of the Atmosphere and Ocean (JISAO) under cooperative agreement NA10OAR4320148, contribution 2366. We greatly appreciate discussions with Thomas P. Ackerman and thank the constructive comments and suggestions of two anonymous reviewers, who clearly helped us to improve the clarity and presentation of the manuscript.

Paul Williams thanks Gerald Mace and one anonymous reviewer for their assistance in evaluating this paper.

References

Alexander, M. J., and L. Pfister (1995), Gravity wave momentum flux in the lower stratosphere over convection, *Geophys. Res. Lett.*, *22*(15), 2029–2032.

Chan, K. R., L. Pfister, T. P. Bui, S. W. Bowen, J. Dean-Day, B. L. Gary, D. W. Fahey, K. K. Kelly, C. R. Webster, and R. D. May (1993), A case study of the mountain lee wave event of January 6, 1992, *Geophys. Res. Lett.*, *20*(22), 2551–2554.

Chan, K. R., J. Dean-Day, S. W. Bowen, and T. P. Bui (1998), Turbulence measurements by the DC-8 meteorological measurement system, *Geophys. Res. Lett.*, *25*(9), 1355–1358.

Deng, M., and G. G. Mace (2006), Cirrus microphysical properties and air motion statistics using cloud radar Doppler moments. Part I: Algorithm description., *J. Appl. Meteorol. Climatol.*, *45*, 1690–1709.

Deng, M., and G. G. Mace (2008), Cirrus cloud microphysical properties and air motion statistics using cloud radar Doppler moments: Water content, particle size, and sedimentation relationships, *Geophys. Res. Lett.*, *35*, L17808, doi:10.1029/2008GL035054.

Gultepe, I., and D. O. Starr (1995), Dynamical structure and turbulence in cirrus clouds: Aircraft observations during FIRE, *J. Atmos. Sci.*, *52*(23), 4159–4181.

Gultepe, I., A. J. Heymsfield, and D. H. Lenschow (1990), A comparison of vertical velocity in cirrus obtained from aircraft and lidar divergence measurements during FIRE, *J. Atmos. Oceanic Technol.*, *7*(1), 58–67.

Harris, F. I. (1977), The effects of evaporation at the base of ice precipitation layers: Theory and radar observations, *J. Atmos. Sci.*, *34*, 651–672.

Heymsfield, A. (1975), Cirrus uncinus generating cells and evolution of cirriform clouds. 2. Structure and circulations of cirrus uncinus generating head, *J. Atmos. Sci.*, *32*(4), 809–819.

Kalesse, H., and P. Kollias (2013), Climatology of high cloud dynamics using profiling ARM Doppler radar observations, *J. Clim.*, *26*, 6340–6359.

Kärcher, B., and U. Lohmann (2002), A parameterization of cirrus cloud formation: Homogeneous freezing including effects of aerosol size, *J. Geophys. Res.*, *107*(D23), 4698, doi:10.1029/2001JD001429.

Kärcher, B., and J. Ström (2003), The roles of dynamical variability and aerosols in cirrus cloud formation, *Atmos. Chem. Phys.*, *3*, 823–838.

Kollias, P., E. E. Clothiaux, M. A. Miller, B. A. Albrecht, G. L. Stephens, and T. P. Ackerman (2007), Millimeter-wavelength radars: New frontier in atmospheric cloud and precipitation research, *Bull. Am. Meteorol. Soc.*, *88*, 1608–1624.

Lenschow, D. H., (1972), The measurement of air velocity and temperature using the NCAR Buffalo Aircraft Measuring System, *Tech. Rep.*, National Center for Atmospheric Research, Boulder, Colo.

Mace, G. G., A. J. Heymsfield, and M. R. Poellot (2002), On retrieving the microphysical properties of cirrus clouds using the moments of the millimeter-wavelength Doppler spectrum, *J. Geophys. Res.*, *107*(D24), 4815, doi:10.1029/2001JD001308.

Muhlbauer, A., T. P. Ackerman, J. M. Comstock, G. S. Diskin, S. M. Evans, R. P. Lawson, and R. T. Marchand (2014), Impact of large-scale dynamics on the microphysical properties of mid-latitude cirrus, *J. Geophys. Res. Atmos.*, *119*, 3976–3996, doi:10.1002/2013JD020035.

Orr, B. W., and R. A. Kropfli (1999), A method for estimating particle fall velocities from vertically pointing Doppler radar, *J. Atmos. Oceanic Technol.*, *16*, 29–37.

Protat, A., and C. R. Williams (2011), The accuracy or radar estimates of ice terminal fall speed from vertically pointing Doppler radar measurements, *J. Appl. Meteorol. Climatol.*, *50*, 2120–2138.

Quante, M., and D. O. Starr (2002), Dynamical processes in cirrus clouds: A review of observational results, in *Cirrus*, edited by M. Quante and D. O. Starr, pp. 346–374, Oxford Univ. Press, New York.

Scott, S. G., T. P. Bui, K. R. Chan, and S. W. Bowen (1990), The meteorological measurement system on the NASA ER-2 Aircraft, *J. Atmos. Oceanic Technol.*, *7*(4), 525–540.

Sreenivasan, K. R. (1995), On the universality of the Kolmogorov constant, *Phys. Fluids*, *7*(11), 2778–2784.

Tennekes, H., and J. L. Lumley (1972), *A First Course in Turbulence*, 300 pp., The MIT Press, Cambridge, Mass.

Welch, P. D. (1967), The use of fast Fourier transform for the estimation of power spectra: A method based on time averaging over short, modified periodograms, *IEEE Trans. Audio Electroacoust.*, *15*, 70–73.

©2014. American Geophysical Union. All Rights Reserved.